

Short communication

## Electrochemical properties of Li–Cr–Mn–O cathode materials for lithium secondary batteries

Kwang-Soo Kim<sup>a</sup>, Seung-Won Lee<sup>a</sup>, Hee-Soo Moon<sup>a</sup>, Hyun-Joong Kim<sup>b</sup>,  
Byung-Won Cho<sup>b</sup>, Won-Il Cho<sup>b</sup>, Jin-Beom Choi<sup>c</sup>, Jong-Wan Park<sup>a,d,\*</sup>

<sup>a</sup> Division of Materials Science and Engineering, Hanyang University, 17 Haengdang-Dong, Seongdong-Gu, Seoul 133-791, South Korea

<sup>b</sup> Nano-Eco Research Center, Korea Institute of Science and Technology, P.O. Box 131, Cheongryang, Seoul 136-791, South Korea

<sup>c</sup> Department of Earth and Environmental Sciences, School of Basic Sciences, Gyeongsang National University, Jinju 660-701, South Korea

<sup>d</sup> Research Center for Energy Conversion and Storage, San 56-1, Shilim-Dong, Kwangak-Gu, Seoul 151-742, South Korea

Received 12 August 2003; accepted 19 November 2003

### Abstract

Layered Li–Cr–Mn–O cathode materials related to the LiCrO<sub>2</sub>–LiMnO<sub>2</sub>–Li<sub>2</sub>MnO<sub>3</sub> solid solution have been synthesized by the mixed-hydroxide method. The materials are characterized by X-ray diffraction (XRD) and electrochemical techniques. The XRD patterns reveal that samples are a solid solution of hexagonal and monoclinic structures. The most promising cathode material in terms of high capacity and stable cycling performance exhibits the average discharge capacity of 204 mAh g<sup>-1</sup> between 2.5 and 4.5 V versus Li/Li<sup>+</sup>.

© 2003 Elsevier B.V. All rights reserved.

**Keywords:** Li<sub>2</sub>MnO<sub>3</sub>; LiCrO<sub>2</sub>; LiMnO<sub>2</sub>; Solid solution; Cathode; Lithium battery

### 1. Introduction

Currently, there is fast-growing demand for a compact power source with high specific energy density and long life for smaller and portable electronic equipment. In order to satisfy these requirements, research on the development of lithium batteries has been intensified. Cathode materials play an important role in determining the performance of lithium-ion batteries.

The Li–Mn–O system has generated a great deal of interest as a cathode material for rechargeable lithium batteries due to its high specific energy, low cost, and low toxicity. Although, layered LiMnO<sub>2</sub> has been proposed as a promising active material for batteries with high performance due to its high theoretic discharge capacity (285 mAh g<sup>-1</sup>), which is nearly twice that of spinel LiMn<sub>2</sub>O<sub>4</sub>, it is difficult to synthesize directly and Jahn–Teller distortion around Mn<sup>3+</sup> causes conversion to a spinel structure during electrochemical cycling [1,2]. Nevertheless, LiMnO<sub>2</sub> may be stabilized as a layer structure by a number of possible substituent elements if appropriate synthetic routes can be developed. New layer-structured cathode materials composed of

lithium, chromium and manganese of various compositions have been reported and has displayed good electrochemical performance [3–8]. Recently, some research groups have produced the layered structure by using a solid solution between Li<sub>2</sub>MnO<sub>3</sub> (Li[Li<sub>1/3</sub>Mn<sub>2/3</sub>]O<sub>2</sub>) and LiMO<sub>2</sub>. Among them, layered Li[Li<sub>0.2</sub>Cr<sub>0.4</sub>Mn<sub>0.4</sub>]O<sub>2</sub> (Li<sub>2</sub>MnO<sub>3</sub>–LiCrO<sub>2</sub>) developed at Pacific Lithium Ltd., contains Li<sup>+</sup>, Cr<sup>3+</sup>, and Mn<sup>4+</sup> in the transition metal layers [9].

In this work, layered Li–Cr–Mn–O systems (LiMnO<sub>2</sub>–LiCrO<sub>2</sub>–Li<sub>2</sub>MnO<sub>3</sub>) have been synthesized using LiOH·H<sub>2</sub>O and Cr–Mn mixed hydroxide by solid-state reaction in air. Mixtures of Cr–Mn mixed hydroxide and various LiOH·H<sub>2</sub>O contents in stoichiometric ratios are ground thoroughly and then calcined at various temperatures in air.

### 2. Experimental

The materials were synthesized by the following solid-state reaction method. Cr(NO<sub>3</sub>)<sub>3</sub>·9H<sub>2</sub>O and Mn(NO<sub>3</sub>)<sub>2</sub>·6H<sub>2</sub>O were used as the starting materials. Cr(NO<sub>3</sub>)<sub>3</sub>·9H<sub>2</sub>O and Mn(NO<sub>3</sub>)<sub>2</sub>·6H<sub>2</sub>O were dissolved in 100 ml of de-ionized water. The pH of the solution was adjusted to a value of 10 by a dropping solution of 6 M NaOH. The resultant metal hydroxide was filtered and dried at 70 °C for 24 h. Mixtures of LiOH·H<sub>2</sub>O and Cr–Mn mixed hydroxide were ground

\* Corresponding author. Tel.: +81-82-2-2290-0386;

fax: +81-82-2-2298-2850.

E-mail address: [jwpark@hanyang.ac.kr](mailto:jwpark@hanyang.ac.kr) (J.-W. Park).

thoroughly (the initial atomic ratio of Li/(Cr + Mn) is designated as  $x$ ) and then calcined at various temperatures (650, 750, 850, 950 °C) in air. The sample was allowed to cool slowly in the furnace to room temperature. Prepared samples were washed to remove trace amounts of  $\text{Li}_2\text{CrO}_4$  with de-ionized water (the color of water-containing  $\text{Li}_2\text{CrO}_4$  is yellow), followed by drying under vacuum at 70 °C.

The phase identification of the synthesized samples was carried out by X-ray diffraction (XRD) analysis with Rigaku Cu  $\text{K}\alpha$  radiation. The scanning rate was 5°/min and the scanning range of diffraction angle ( $2\theta$ ) was  $10^\circ \leq 2\theta \leq 90^\circ$ . The morphologies of the samples were observed using a field emission scanning electron microscopy (FESEM), JSM-6400F.

The cathode slurry contained active material, acetylene black as conductor and PTFE binder in a weight ratio of 75:10:15. The electrochemical cell was comprised of the prepared samples as a positive electrode, Li foil as a negative electrode, and an electrolyte of 1 M solution of  $\text{LiPF}_6$  in ethylene carbonate (EC)–dimethyl carbonate (DMC) (1:1, v/v). The cell was assembled in an argon-filled dry box.

The assembled cell was cycled galvanostatically at 25  $\text{mA g}^{-1}$  between 2.5 and 4.5 V using a battery cycler. Cyclic voltammetry measurements were carried out at a scan rate of 0.07  $\text{mV s}^{-1}$ .

### 3. Results and discussion

#### 3.1. Effect of lithium content

The XRD patterns of sample ( $x = 1.4, 1.55, 1.63$  and  $1.71$ ) prepared at 850 °C are shown in Fig. 1. The spectra indicate that all the peaks are indexable for a layered structure based on hexagonal  $\alpha\text{-NaFeO}_2$ , which is characteristic

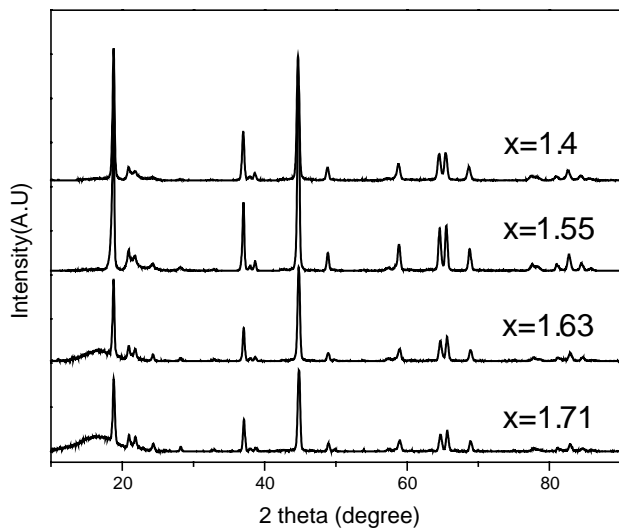


Fig. 1. XRD pattern of Li–Cr–Mn–O compounds ( $x = 1.4, 1.55, 1.63$  and  $1.71$ ) prepared at 850 °C.

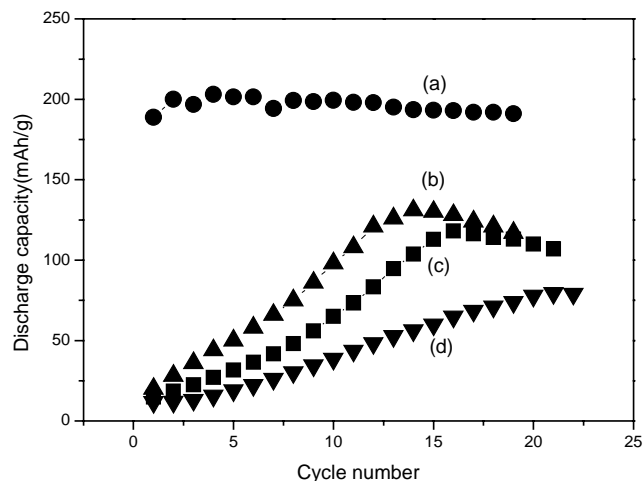


Fig. 2. Cycling performance of samples prepared at 850 °C in the voltage range of 2.5–4.5 V at a constant current density of 25  $\text{mA g}^{-1}$ : (a)  $x = 1.4$ ; (b)  $x = 1.55$ ; (c)  $x = 1.63$ ; (d)  $x = 1.71$ .

of layered structures such as  $\text{LiCoO}_2$  and  $\text{LiMnO}_2$ , except for the peaks between 20° and 35° which show a  $\text{Li}_2\text{MnO}_3$  (monoclinic phase) character. The more the lithium content increases, the more monoclinic peak of XRD pattern tends to become sharp and strong. It is concluded that the monoclinic structure  $\text{Li}_2\text{MnO}_3$  increases as the lithium hydroxide content increases. Zhang and Noguchi [10] have reported that a layered Li–Cr–Ti–O compound synthesized in air contains an impurity phase,  $\text{Li}_2\text{CrO}_4$ . This indicates that lithium plays an important role in a layered monoclinic solid-solution structure as well as in its composition because lithium and chromium are consumed as impurity phases.

The cycling performance of the Li–Cr–Mn–O compound calcined at 850 °C in air is shown in Fig. 2. Electrochemical studies were performed galvanostatically in the voltage range 2.5–4.5 V at a constant current density of 25  $\text{mA g}^{-1}$ . The sample with  $x = 1.55$  shows a discharge capacity of 189  $\text{mAh g}^{-1}$  on the 1st cycle and 198  $\text{mAh g}^{-1}$  on the 10th cycle. The maximum discharge capacity is 204  $\text{mAh g}^{-1}$  at cycle 4. The discharge capacity of the other compounds increases upon cycling until the maximum capacity is reached. It is considered that this phenomenon occurs because of structural re-ordering or a decrease in cell resistance on cycling. Additional research is needed to explain this phenomenon.

#### 3.2. Effect of calcining temperature

A study of the effect of calcining temperature was performed in order to understand the effect of various temperatures because it plays an important role in morphology and crystallinity. The most promising samples, i.e., those with  $x = 1.55$  (chemical composition result:  $\text{Li}_{1.13}\text{Cr}_{0.15}\text{Mn}_{0.73}\text{O}_2$ ) were calcined at 650, 750, 850 and 950 °C for 14 h in air. The XRD patterns of samples calcined at each temperature are shown in Fig. 3. The data

indicate that all peaks are indexable for a layered structure based on hexagonal  $\alpha\text{-NaFeO}_2$  except for peaks between  $20^\circ$  and  $35^\circ$  with  $\text{Li}_2\text{MnO}_3$  (monoclinic phase) character, as observed earlier for samples prepared with different lithium hydroxide contents. In the XRD spectra, the arrow is the (111) peak of monoclinic  $\text{Li}_2\text{MnO}_3$ . The more the calcining temperature is increased, the more the monoclinic (111) peak becomes sharp and strong.

The variation in the grain size of a Li–Cr–Mn–O compound ( $x = 1.55$ ) prepared under various calcining temperatures is shown in Fig. 4. The grain size increases from 100 nm to  $1\ \mu\text{m}$  as the calcining temperature is increased. The particle size is irregular in the sample calcined at  $950^\circ\text{C}$ .

The variation in discharge capacity with cycle number for Li–Cr–Mn–O ( $x = 1.55$ ) calcined at various temperatures is presented in Fig. 5. Cycling tests were carried out galvanostatically at  $25\ \text{mA g}^{-1}$  between 2.5 and 4.5 V. The sample with  $x = 1.55$  yields a discharge capacity of  $189\ \text{mAh g}^{-1}$  on the 1st cycle and  $198\ \text{mAh g}^{-1}$  on the 10th cycle. For samples calcined at 650 and  $750^\circ\text{C}$ , the discharge capacity increases at the beginning and then decreases rapidly. The discharge capacity of the sample prepared at  $950^\circ\text{C}$  increase initially and then remains constant from the 10th cycle onwards.

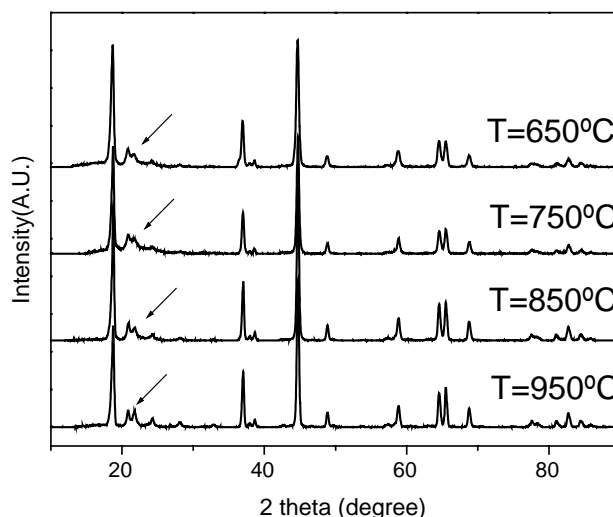


Fig. 3. XRD patterns of samples ( $x = 1.55$ ) calcined at 650, 750, 850 and  $950^\circ\text{C}$  for 14 h.

The charge–discharge curve and cyclic voltammogram of samples with  $x = 1.55$  calcined at various temperatures are shown in Figs. 6 and 7, respectively. All samples display a capacity loss that is attributable to the irreversible

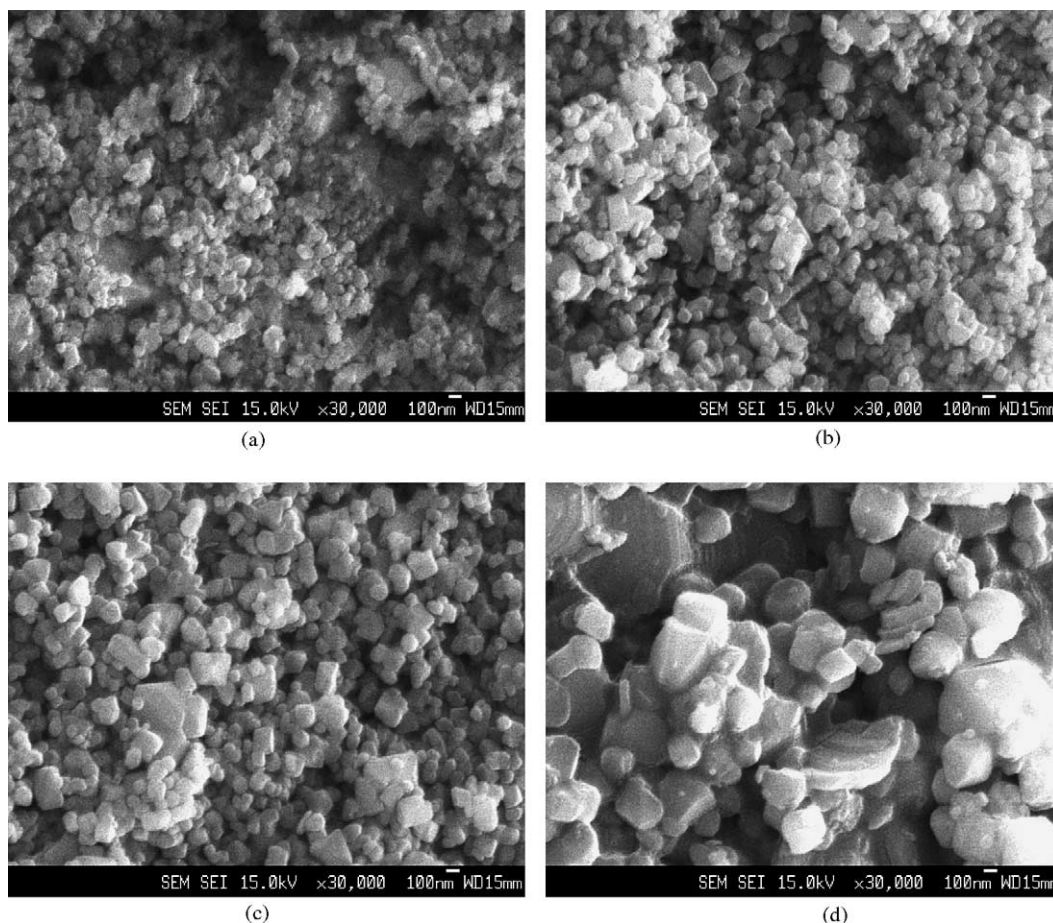


Fig. 4. Scanning electron micrograph of Li–Cr–Mn–O ( $x = 1.55$ ) calcined at various temperatures: (a)  $650^\circ\text{C}$ ; (b)  $750^\circ\text{C}$ ; (c)  $850^\circ\text{C}$ ; (d)  $950^\circ\text{C}$ .

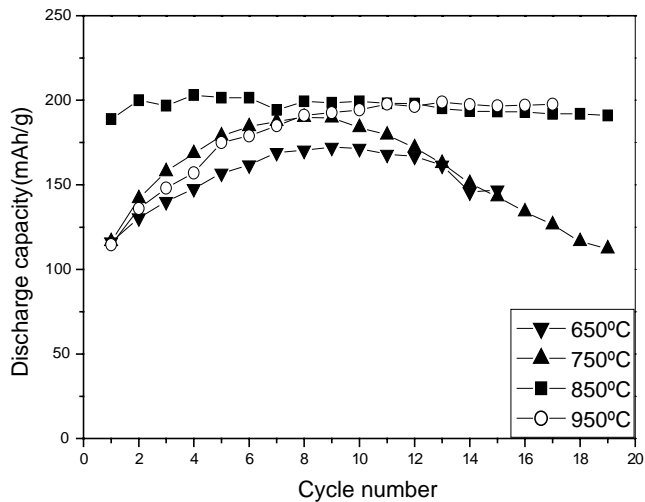


Fig. 5. Cycling performance of Li-Cr-Mn-O ( $x = 1.55$ ) prepared at various temperatures in voltage range 2.5–4.5 V at a constant current density of  $25 \text{ mA g}^{-1}$ .

reaction between first charge and discharge (Fig. 6). The charge–discharge curves for the first and second cycles have different shapes, except for the sample calcined at  $850^\circ\text{C}$ . The gradual increase of capacity (Fig. 5) is attributed either to a phase transition in the samples or a decrease in cell resistance. The first charging scan of samples shows a strong peak at about 3.9 V (Fig. 7). This appears to be related to  $\text{Cr}^{3+/6+}$  oxidation [11]. In contrast with other samples

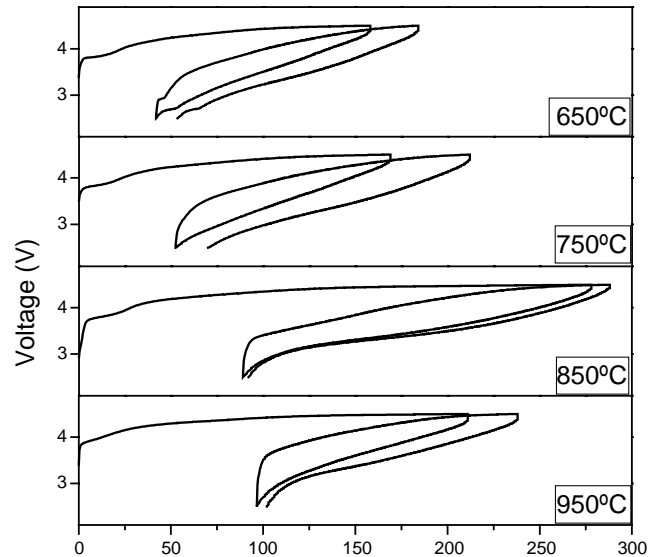


Fig. 6. Charge–discharge curve of samples ( $x = 1.55$ ) calcined at various temperatures between 2.5 and 4.5 V using a constant current of  $25 \text{ mA g}^{-1}$ .

(Fig. 6), the sample calcined at  $650^\circ\text{C}$  displays a transition curve at low voltage (around 2.7 V) during subsequent cycling. These plateaux can be strongly supported by the cyclic voltammogram, as shown in Fig. 7. These peaks (2.9/2.7 V) in the low-voltage region are probably related to the voltage profile (below 3 V) of  $m\text{-LiCr}_x\text{Mn}_{1-x}\text{O}_2$  [12]. The 4.5 V peak intensity (oxygen loss peak) of the sample calcined at

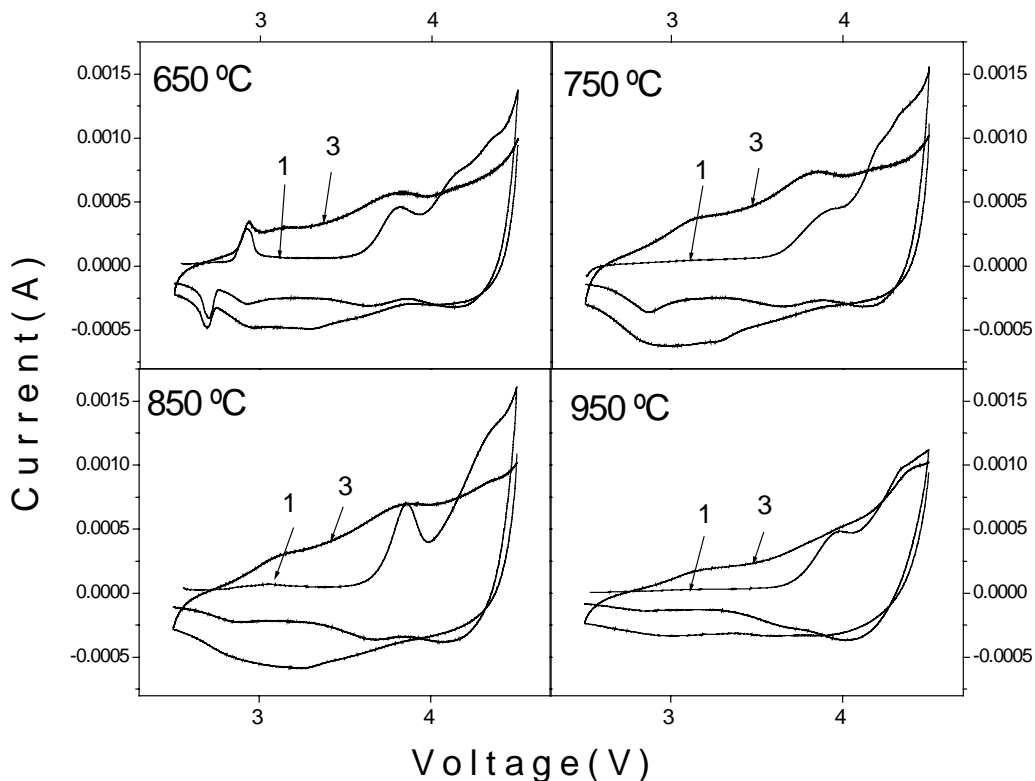


Fig. 7. Cyclic voltammogram of samples with  $x = 1.55$  calcined at various temperatures (scan rate =  $0.07 \text{ mV s}^{-1}$ ).

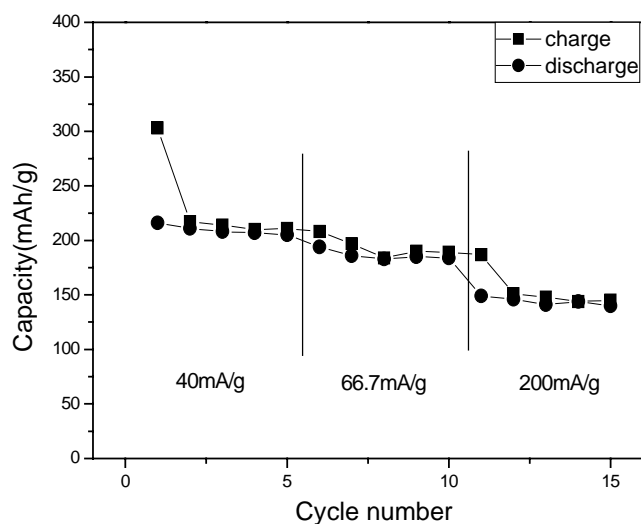


Fig. 8. Capacity vs. cycle number of a sample ( $x = 1.55$ ) calcined at  $850\text{ }^{\circ}\text{C}$  for indicated current densities.

$950\text{ }^{\circ}\text{C}$  is smaller than those of the other samples and remains constant upon cycling (Fig. 7). This is consistent with the results reported by Kim et al. [13].

Plots of capacity versus cycle number for a sample with  $x = 1.55$  calcined at  $850\text{ }^{\circ}\text{C}$  at various discharge currents are presented in Fig. 8. The cell was charged using a current of  $25\text{ mA g}^{-1}$  for all cycles and discharged using a current of 40, 66.7 and  $200\text{ mA g}^{-1}$  at intervals of five cycles between 2.5 and 4.5 V. The cell still had a discharge capacity of over  $140\text{ mAh g}^{-1}$  at  $200\text{ mA g}^{-1}$  after 10 cycles.

#### 4. Conclusions

Layered Li–Cr–Mn–O cathode materials related to the  $\text{LiCrO}_2\text{--LiMnO}_2\text{--Li}_2\text{MnO}_3$  solid solution have been synthesized. The XRD patterns show that samples are a solid

solution of hexagonal and monoclinic structures. During electrochemical charge–discharge cycling, with the exception of the sample with  $x = 1.55$  and calcined at  $850\text{ }^{\circ}\text{C}$ , the initial discharge capacity of all samples increases during cycling and then decreases rapidly. Additional research is required to explain this phenomenon. A sample with  $x = 1.55$  and calcined at  $850\text{ }^{\circ}\text{C}$  gives a discharge capacity of  $204\text{ mAh g}^{-1}$  at a constant current of  $25\text{ mA g}^{-1}$  and also good cycling performance at high current. From these results, the Li–Cr–Mn–O system is regarded as a promising cathode material.

#### Acknowledgements

This work was supported by KOSEF through the Research Center for Energy Conversion and Storage.

#### References

- [1] G. Vitins, K. West, J. Electrochem. Soc. 144 (1997) 2587.
- [2] Y.-I. Jang, B. Huang, Y.-M. Chiang, D.R. Sadoway, Electrochem. Solid State Lett. 1 (1998) 13.
- [3] J. Cho, B. Park, Electrochem. Solid State Lett. 3 (2000) 355.
- [4] J. Cho, Y.J. Kim, B. Park, Solid State Ionics 138 (2001) 221.
- [5] C. Storey, I. Kargina, Y. Grincourt, I.J. Davidson, Y.C. Yoo, D.Y. Seung, J. Power Sources 97–98 (2001) 541.
- [6] Y. Grincourt, C. Storey, I.J. Davidson, J. Power Sources 97–98 (2001) 711.
- [7] M. Balasubramanian, J. McBreen, I.J. Davidson, P.S. Whitfield, I. Kargina, J. Electrochem. Soc. 149 (2002) A176.
- [8] B. Ammundsen, J. Paulsen, I. Davidson, R.-S. Liu, C.-H. Shen, J.-M. Chen, L.-Y. Jang, J.-F. Lee, J. Electrochem. Soc. 149 (2002) A431.
- [9] B. Ammundsen, J. Paulsen, Adv. Mater. 13 (2001) 943.
- [10] L. Zhang, H. Noguchi, J. Electrochem. Soc. 150 (2003) A601.
- [11] Z. Lu, J.R. Dahn, J. Electrochem. Soc. 149 (2002) A1454.
- [12] Z.P. Guo, G.X. Wang, H.K. Liu, S.X. Dou, Solid State Ionics 148 (2002) 359.
- [13] J.-H. Kim, C.S. Yoon, Y.-K. Sun, J. Electrochem. Soc. 150 (2003) A538.